Development 130, 4123-4133

doi:10.1242/dev.00559

Altered fracture repair in the absence of MMP9

Céline Colnot[1], Zachary Thompson[1], Theodore Miclau[1], Zena Werb[2] and Jill A. Helms[1,*]

[1]Department of Orthopaedic Surgery, University of California, San Francisco, California, 94143-0514
[2]Department of Anatomy, University of California, San Francisco, California, 94143-0514
*Author for correspondence (e-mail: helms@itsa.ucsf.edu)

Accepted 22 April 2003

SUMMARY

The regeneration of adult skeletal tissues requires the timely recruitment of skeletal progenitor cells to an injury site, the differentiation of these cells into bone or cartilage, and the re-establishment of a vascular network to maintain cell viability. Disturbances in any of these cellular events can have a detrimental effect on the process of skeletal repair. Although fracture repair has been compared with fetal skeletal development, the extent to which the reparative process actually recapitulates the fetal program remains uncertain. Here, we provide the first genetic evidence that matrix metalloproteinase 9 (MMP9) regulates crucial events during adult fracture repair. We demonstrate that MMP9 mediates vascular invasion of the hypertrophic cartilage callus, and that *Mmp9*$^{-/-}$ mice have non-unions and delayed unions of their fractures caused by persistent cartilage at the injury site. This MMP9-dependent delay in skeletal healing is not due to a lack of vascular endothelial growth factor (VEGF) or VEGF receptor expression, but may instead be due to the lack of VEGF bioavailability in the mutant because recombinant VEGF can rescue *Mmp9*$^{-/-}$ non-unions. We also found that *Mmp9*$^{-/-}$ mice generate a large cartilage callus even when fractured bones are stabilized, which implicates MMP9 in the regulation of chondrogenic and osteogenic cell differentiation during early stages of repair. In conclusion, the resemblance between *Mmp9*$^{-/-}$ fetal skeletal defects and those that emerge during *Mmp9*$^{-/-}$ adult repair offer the strongest evidence to date that similar mechanisms are employed to achieve bone formation, regardless of age.

Key words: Matrix metalloproteinase 9, Vascular endothelial growth factor, Endochondral ossification, Cartilage, Bone healing, Mechanical environment, Mouse

INTRODUCTION

The bony skeleton possesses an astounding regenerative potential. Unlike other adult tissues, which generate scar tissue at the site of an injury, the skeleton heals by forming new bone that is indistinguishable from adjacent, uninjured tissue. There are aspects of this adult regenerative process that bear a resemblance to fetal skeletal tissue development. For example, both fetal and adult skeletal progenitor cells aggregate to form cell condensations that eventually differentiate into skeletal tissue (Hall, 1988; Thompson et al., 2002). The same molecular markers of chondrogenesis and osteogenesis are expressed during development and repair, which suggests that the regulation of cell differentiation is also conserved (Ferguson et al., 1999; Karsenty and Wagner, 2002; Vortkamp et al., 1998). In both processes, vascularization is a prerequisite for ossification (Thompson et al., 2002; Vu et al., 1998), and disruptions in extracellular matrix remodeling can delay subsequent bone formation.

There are also notable differences between the adult reparative process and fetal skeletal development. For example, mechanical forces have not been implicated in the initiation of chondrogenesis or osteogenesis during fetal development, but the role of the mechanical environment during adult repair (Carter et al., 1998; Probst and Spiegel, 1997), and its effect on cartilage and bone formation during fracture healing (Le et al., 2001; Thompson et al., 2002) has been well documented. An inflammatory reaction exerts a substantial effect on adult skeletal repair (Simon et al., 2002), whereas the immune system has no known role in fetal skeletogenesis. Likewise, skeletal progenitor cells abound in the fetus, whereas they may be limited in number in the adult (Bruder et al., 1994; Ekholm et al., 2002).

We found the parallels between fetal skeletal development and adult repair particularly intriguing, and pursued this issue in the context of fracture healing. Our investigation focused on the extent to which the functions of one molecule, matrix metalloproteinase 9 (MMP9), were equivalent during skeletal development and fracture healing. We developed several novel models of skeletal repair, and exploited the *Mmp9*$^{-/-}$ mouse in order to gain the first molecular insights into the regulation of angiogenesis during skeletal tissue regeneration.

MATERIALS AND METHODS

Non-stabilized and stabilized fractures

Mmp9$^{-/-}$ mice [3- to 5-month old; 30-35 grams (g)] and their wild-type littermates were anesthetized with an intraperitoneal injection of 2% Avertin (0.015 ml/g body weight). Closed, standardized non-

stable fractures were produced following protocols approved by the UCSF Committee on Animal Research. The tibia was placed on the fracture jig and 460 g weight was dropped from 14 cm to create a closed, transverse fracture by three-point bending, which was confirmed by radiography. These non-stabilized fractures heal through the formation of a cartilage intermediate (Thompson et al., 2002). To produce stabilized fractures, which heal without a cartilage intermediate, an external fixation device was placed at the time of fracture (Tay et al., 1998; Thompson et al., 2002). Mice with non-stabilized fractures were sacrificed by cervical dislocation following deep inhalation anesthesia (Metofane) at 3 (n=6), 6 (n=6), 10 (n=10), 14 (n=19), 21 (n=6) and 28 (n=6) days post-fracture. Mice with stabilized fractures were sacrificed at 3 (n=6), 7 (n=8), 10 (n=11), 14 (n=16), 21 (n=10) and 28 (n=10) days post-fracture.

Pin implantation

Mice were anesthetized as described above. Using a percutaneous approach, stainless steel pins (0.25mm diameter) were inserted through the marrow and both tibial cortices; pin ends were cut flush with the skin. Mice were sacrificed 7 and 10 days after surgery, and pins were removed from the tibiae following decalcification.

Treatment with recombinant vascular endothelial growth factor (VEGF) protein

Mmp9$^{-/-}$ tibiae were fractured as described above and recombinant vascular endothelial growth factor (rVEGF) protein (5.0 μg/injection; Genentech) was delivered at four separate time-points (6, 7, 8 and 9 days post-fracture). Following inhalation anesthesia, percutaneous injections were made directly into the fracture site using a 30 gauge needle. Extreme care was taken to avoid displacing the bone ends during these injections. Control *Mmp9*$^{-/-}$ mice received injections of an equivalent volume of vehicle (PBS) at the same time-points. PBS and rVEGF-injected mice were sacrificed at 10 (n=5 PBS-injected, n=5 rVEGF-injected) and 14 (n=5 PBS-injected, n=5 rVEGF-injected) days post-fracture.

Biomechanical analyses (distraction to failure testing)

Closed tibial fracture tissues were collected at 14 and 19 days post-fracture. The tibiae were carefully dissected free of surrounding soft tissue, placed in normal saline and stored overnight at 4°C. The tibiae were prepared for mechanical testing by placing 0.25 mm transfixion pins (Fine Science Tools, Foster City, CA) into the bone at locations that were proximal and distal to the fracture site. The proximal and distal ends of the bone, including the pins, were embedded in polymethylmethacrylate (PMMA), leaving the fracture callus exposed. Tissues were kept moist until they were loaded onto the materials testing system (Bionix 858; MTS, Eden Prairie, MN) with a precision force transducer (100# [454 N] Load Cell Model 31, Sensotec, Columbus, OH). The ends of the bone were secured to the machine using a custom-made clamp. The tibiae were then loaded in distraction at a rate of 0.25 mm/minute with simultaneous force and displacement data recorded. Maximum force at failure (in Newtons, N) was calculated for each specimen.

Histology and immunohistochemistry

Under RNase-free conditions, callus tissues were fixed overnight at 4°C in 4% paraformaldehyde. Callus tissues were decalcified at 4°C in 19% EDTA (pH 7.4) for 10-14 days, then dehydrated in a graded ethanol series and embedded in paraffin. The entire callus was sectioned (10 μm thick), and adjacent sections were analyzed using a variety of histological and cellular analyses. Safranin-O/Fast Green (SO) staining was performed as described (Thompson et al., 2002). Trichrome staining was performed to analyze bone formation in the fracture callus, the Aniline Blue (AB) component of the trichrome stain was selected for image analyses. Tartrate resistant acid phosphatase (TRAP) staining was performed using a leukocyte acid phosphatase kit (Sigma, St. Louis, MO). For platelet endothelial cell adhesion molecule (PECAM)- and MMP9-antibody staining, sections were de-paraffinized, immersed in 5% H_2O_2/PBS for 5 minutes, washed in PBS, treated with 0.1 M glycine for 30 seconds, washed in PBS, and then incubated in the following blocking solutions followed by intermediate PBS washes: 5% powdered milk for 10 minutes; 1.0 mg/ml ovalbumin for 10 minutes; and 5% sheep serum for 30 minutes. Sections were incubated overnight at 4°C in monoclonal rat anti-mouse PECAM1 (BD PharMingen, San Diego, CA) or a polyclonal rabbit anti-mouse MMP9, washed in PBS, blocked in 5% sheep serum for 30 minutes, and incubated for 1 hour at room temperature in biotinylated anti-rat IgG (BD PharMingen, San Diego, CA) or biotinylated anti-rabbit IgG (Jackson Immunoresearch). Slides were washed in PBS and incubated in horseradish peroxidase-conjugated streptavidin (Amersham, Cleveland, OH). Signal was revealed by incubation in a diaminobenzidine solution containing 1% $CoCl_2$ and 1% Ni_3SO_4 for PECAM immunostaining (Vu et al., 1998). For MMP9-TRAP double staining, TRAP staining was performed following MMP9 immunostaining.

In situ hybridization

In situ hybridization was performed using mouse cDNAs for *Mmp9*, *ColIIa* (*Col2a1* – Mouse Genome Informatics), *ColX* (*Col10a1* – Mouse Genome Informatics), *Oc* (*Tcirg1* – Mouse Genome Informatics), *Vegf* (*Vegfa* – Mouse Genome Informatics), and the Vegf receptors *Flk-1*, *Flt1* (*Kdr* – Mouse Genome Informatics) and neuropilin 2. Sections were de-waxed, fixed in 4% PFA, treated with 20.0 μg/ml Proteinase K, fixed with 4% PFA, incubated in 0.1% sodium borohydride/PBS and acetylated in a solution of 0.1 M triethanolamine-HCl. Sections were then hybridized with ^{35}S-labeled denatured probes overnight at 45°C. Sections were then washed in 5×SSC containing 20 mM β-mercaptoethanol at 45°C, then in 50% formamide containing 2×SSC at 45°C, followed by a wash in 2×SSC, and lastly in 0.1×SSC at room temperature. Sections were then dehydrated in a graded ethanol series. Emulsion coating was performed as described (Albrecht et al., 1997). Image analyses were performed as described previously (Ferguson et al., 1999).

Histomorphometric measurements

At 10 and 14 days, the fracture callus was composed of cartilage, islands of bone, and fibrous tissue. To determine the volume of the callus and the cartilage within each callus, and to circumvent difficulties in assessing a heterogenous tissue such as the fracture callus, we first sectioned the entire callus. From the resulting 300 tissue sections (each 10 μm in thickness), histomorphometric analyses were performed. In our initial studies we analyzed tissue sections every 30 μm; we later determined that tissue sections taken at a 300 μm interval produced the same results. Thus, for each callus, an average of 10-15 tissue sections were used to determine callus and cartilage volumes. Sections were stained with SO and images of each section were photographed using a digital camera. Images were imported into Adobe PhotoShop, and the software was used to quantify the area of the callus and the area of cartilage (which stained red after SO histological analysis). The areas of the callus and the cartilage were both determined empirically in a double-blinded manner, and checked by an independent investigator. These data were used to calculate the total volume of each callus and the total volume of cartilage in each callus.

RESULTS

MMP9 is expressed throughout the entire process of adult skeletal regeneration

The initial stage of fracture healing is characterized by an acute inflammatory reaction, which has been proposed to stimulate mesenchymal cell proliferation at the site of injury (Einhorn et

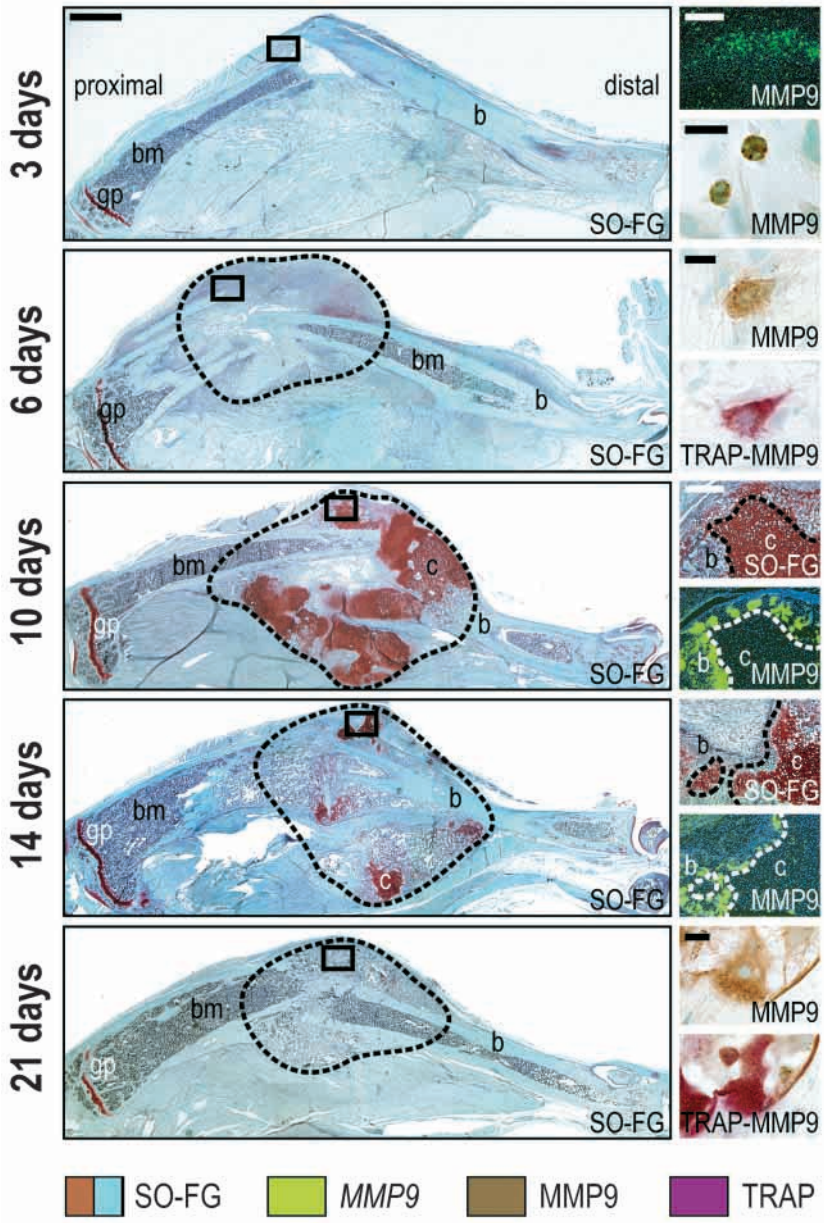

Fig. 1. MMP9 expression during non-stable fracture healing. (Left column) Sagittal sections through the wild-type callus at 3, 6, 10, 14 and 21 days post-fracture, stained with Safranin-O/Fast Green (SO-FG), illustrates the abundant proteoglycan-containing cartilage (red, c) that appears during the soft callus phase of healing (4-10 days post-fracture) and is resorbed during the hard callus phase of healing (10-21 days post-fracture). The borders of the fracture callus are delimited with a dotted line. The proximal half of the broken tibia is on the left side, showing the growth plate, and the distal part of the tibia is on the right side. (Right column) In situ hybridization and immunostaining analyses at 3, 6, 10, 14 and 21 days post-fracture. At 3 days, analyses show *Mmp9* mRNA (green) and MMP9 protein (brown) in inflammatory cells around the fracture site. At 6 days, MMP9 protein is detected in TRAP-positive cells at the fracture site. At 10 days, *Mmp9* mRNA is localized to cells at the boundary between the cartilage callus (c) and newly forming bone (b). This cartilage-bone boundary, demarcated by a dotted line, is visualized with SO-FG staining on an adjacent section. At 14 days, *Mmp9*-expressing cells are detected at the site of hypertrophic cartilage degradation. At 21 days, MMP9- and TRAP-positive osteoclasts are localized in the callus at the site of new bone remodeling. Higher magnifications in the right column correspond to the boxed areas in the left column. gp, growth plate; bm, bone marrow; b, bone. Scale bars: SO-FG staining (low magnification), 2 mm; SO-FG staining (high magnification) and *Mmp9* in situ hybridization, 250 μm; MMP9 immunostaining and TRAP-MMP9 double staining, 10 μm.

al., 1995). In mice, this inflammatory period encompasses the first 3-4 days post-fracture (Le et al., 2001). During this window of time, we noted abundant *Mmp9* mRNA and MMP9 protein expression in mesenchymal and inflammatory cells surrounding the fracture site (Fig. 1, 3 days). The inflammatory stage is closely followed by the soft callus phase of repair, during which time mesenchymal cells differentiate into chondrocytes and begin their maturation process to a state of hypertrophy. In mice, this stage lasts up to 10 days post-fracture and is characterized by the formation of a cartilage callus that acts to stabilize the fractured bone ends (Le et al., 2001). During the early part of the soft callus phase, a large number of MMP9-positive and TRAP-positive preosteoclasts were detected at the fracture site (Fig. 1, 6 days). During the latter part of the soft callus phase we noted that *Mmp9* expression in osteoclasts/chondroclasts interposed between the hypertrophic cartilage and the newly forming bone of the fracture callus (Fig. 1, 10 days; and Fig. 5A).

The hard callus phase of repair is characterized by the replacement of a cartilage scaffold with bone, and this occurs between 10 and 21 days post-fracture in mice (Le et al., 2001). At 14 days, MMP9-positive cells were found within the hypertrophic cartilage callus localized to sites of vascular invasion (Fig. 1, 14 days; and Fig. 5). During the remodeling phase of healing, which in mice extends from 14 days post-fracture until a minimum of two weeks afterwards, MMP9 was strongly expressed in osteoclasts that were in the process of degrading new bone matrix (Fig. 1, 21 days).

Mmp9$^{-/-}$ mice display abnormal fracture healing

Given the expression of MMP9 throughout the course of bone repair, we speculated that some aspect of adult skeletal repair would be compromised in *Mmp9*$^{-/-}$ mice. The most obvious difference we noted was during the hard callus phase of repair. Whereas the wild-type cartilage callus was undergoing rapid degradation and remodeling by 14 days, the *Mmp9*$^{-/-}$

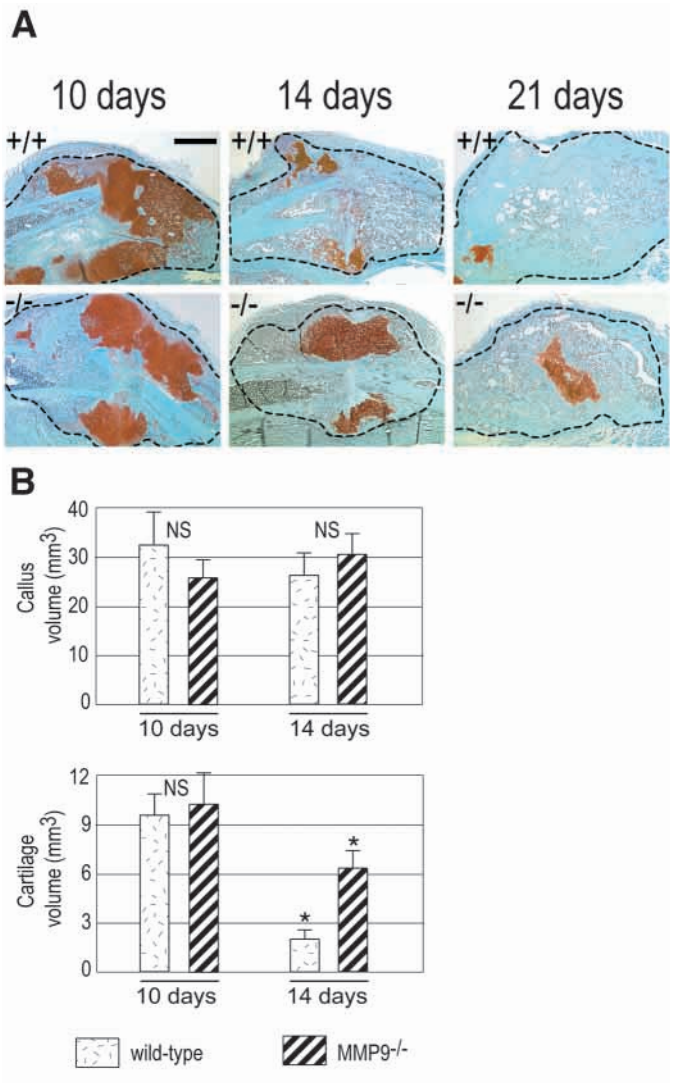

Fig. 2. *Mmp9*$^{-/-}$ mice exhibit an accumulation of cartilage during non-stable fracture healing. (A) SO-FG staining of wild-type (top, +/+) and *Mmp9*$^{-/-}$ callus tissues (bottom, –/–) at 10, 14 and 21 days indicates that cartilage persists in the *Mmp9*$^{-/-}$ callus up to 21 days. (B) Histomorphometric measurements of total callus and cartilage volumes in wild-type (n=12) and *Mmp9*$^{-/-}$ (n=17) mice at 10 and 14 days. There is a statistically significant increase in the volume of cartilage in *Mmp9*$^{-/-}$ calluses compared with wild-type calluses at 14 days (asterisks, Student's t-test, P=0.02). Bars represent mean±s.e.m. Scale bar: 1 mm.

callus was apparently resistant to degradation (Fig. 2A,B). Histomorphometric analyses confirmed these observations, and revealed that *Mmp9*$^{-/-}$ calluses comprised almost three times more cartilage than wild-type calluses (Fig. 2B). The healing defect in *Mmp9*$^{-/-}$ mice persisted into the latter part of the hard callus stage; long after wild-type cartilage had been replaced by bone, the *Mmp9*$^{-/-}$ callus still exhibited residual cartilage islands (Fig. 2A, 21 days). By the remodeling phase (e.g. 28 days), *Mmp9*$^{-/-}$ and wild-type calluses were both composed primarily of bone (data not shown), indicating that the *Mmp9*$^{-/-}$ repair defect was reversible. We had observed a similar reversal in the *Mmp9*$^{-/-}$ fetal skeletal defect around the time of puberty in the mouse (Vu et al., 1998).

The *Mmp9*$^{-/-}$ mutation affects cartilage remodeling but not chondrocyte maturation

One possible explanation for the *Mmp9*$^{-/-}$ repair defect we had observed was that *Mmp9*$^{-/-}$ chondrocytes were slower to mature, and that this ultimately affected their rate of fracture repair. We tested this hypothesis by examining chondrocyte maturation in wild-type and mutant mice at numerous time-points during the healing process. At 7 and 10 days post-fracture, most wild-type callus chondrocytes expressed mRNA for collagen type IIa (*ColIIa*), a marker of resting, proliferating and mature chondrocytes (Sandell et al., 1997). The same was true of chondrocytes in the *Mmp9*$^{-/-}$ callus (data not shown). Likewise, the area of collagen type X (*ColX*) expression, a marker of hypertrophic chondrocytes (Hiltunen et al., 1993), was equivalent in wild-type and *Mmp9*$^{-/-}$ calluses (Fig. 3), indicating that the *Mmp9*$^{-/-}$ mutation did not affect the transition of chondrocytes from a mature to a hypertrophic state.

By sharp contrast, the removal of hypertrophic *ColX*-expressing cartilage was profoundly affected in *Mmp9*$^{-/-}$ mice (Fig. 3). We noted that in wild-type mice, the *ColX* domain was much smaller at 14 days than at 10 days post-fracture, indicating that the onset of hypertrophic cartilage degradation began between these two time points (Fig. 3). However, in *Mmp9*$^{-/-}$ mice the *ColX* domain remained large, even after 14 days (Fig. 3). Thus, MMP9 was not required for chondrocyte maturation but it did play a role in the degradation and removal of hypertrophic cartilage. Once again, this phenotype bore a striking resemblance to the defect we had observed during fetal development (Vu et al., 1998).

The *Mmp9*$^{-/-}$ mutation affects the biomechanical properties of the fracture callus

A crucial aspect of bone healing is that the regenerated tissue must provide sufficient strength to the injured limb in order for the animal to regain function. We sought to determine if the *Mmp9*$^{-/-}$ mutation compromised the strength and stability of an injured bone. We first used a biomechanical test to measure callus strength. We chose the distraction-to-failure model as a mode of testing because the geometry of a non-stabilized fracture is highly variable, which renders more standard biomechanical tests less accurate. Wild-type and *Mmp9*$^{-/-}$ calluses were subjected to a gradual distractive force and the maximum force required to cause rupture of the callus was determined (White et al., 1977). At 14 days, we found the maximum force at failure was greater in wild-type [5.19±0.63 Newtons (N), ±s.e.m.; n=8] than in *Mmp9*$^{-/-}$ calluses (4.29±1.06 N; n=13; P=0.045, Student's t-test), indicating that *Mmp9*$^{-/-}$ calluses were structurally weaker than wild-type calluses. By 19 days, the maximum force at failure was equivalent in wild-type (6.99±1.22 N, n=11) and *Mmp9*$^{-/-}$ calluses (6.47±0.97 N; n=10; P=0.41), which supported our previous observations that the *Mmp9*$^{-/-}$ defect resolved around the onset of bony remodeling. Collectively, these data indicate that MMP9 serves at least two functions during skeletal tissue regeneration. First, MMP9 is necessary for the efficient degradation and remodeling of the hypertrophic cartilage callus. Second, MMP9 participates in the regeneration of osseous tissue in the callus. Ultimately, these data indicate that MMP9 activity is crucial for the regeneration of functional skeletal tissue.

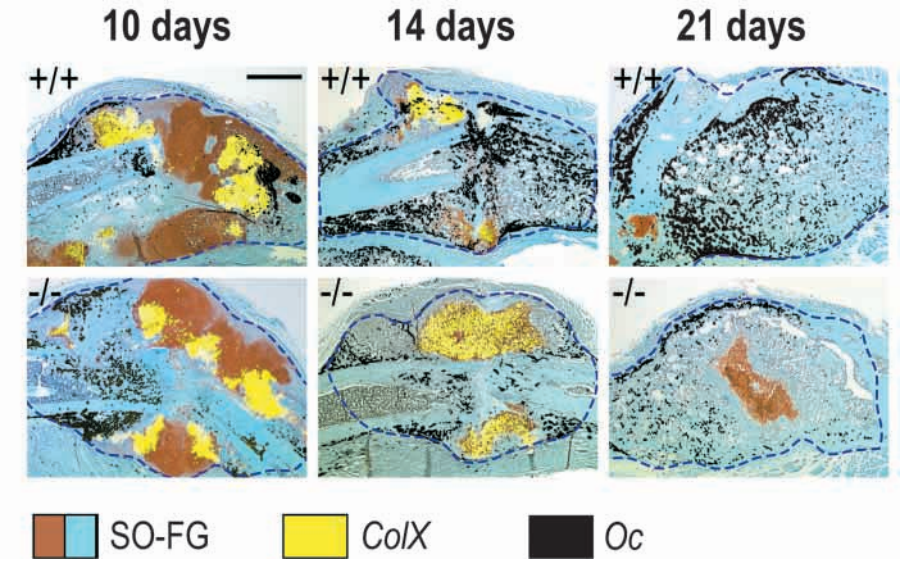

Fig. 3. Hypertrophic callus remodeling and bone formation are delayed in *Mmp9*$^{-/-}$ mice. Transcripts for collagen type X (*ColX*, yellow) and osteocalcin (*Oc*, black) are superimposed onto adjacent sections stained with SO-FG to illustrate the location of hypertrophic cartilage and new bone (same sections showing only SO-FG staining are also shown in Fig. 2B). By 14 days, *ColX* (yellow) is downregulated in the wild-type callus but remains strongly expressed throughout the *Mmp9*$^{-/-}$ callus. Conversely, *Oc* is strongly expressed in the wild-type callus by 14 days but is expressed at much lower levels in the *Mmp9*$^{-/-}$ callus. Blue dotted lines represent the boundary of the callus. Scale bar: 1 mm.

The *Mmp9*$^{-/-}$ mutation impairs ossification during fracture healing

Our previous analyses of the cranial and appendicular skeletons of prenatal and early postnatal *Mmp9*$^{-/-}$ mice had failed to reveal defects in intramembranous ossification (Vu et al., 1998). However, in our fracture healing model we had observed that intramembranous ossification was disrupted. Using osteocalcin (*Oc*) expression as an indicator of osteogenesis (Lian et al., 1978), we ascertained that *Oc* was expressed at very low levels, and only at the periphery of the callus, in *Mmp9*$^{-/-}$ mice, whereas *Oc* was expressed throughout wild-type calluses by day 14 (Fig. 3). This retardation in intramembranous ossification persisted in *Mmp9*$^{-/-}$ mice into the remodeling phase of fracture repair (Fig. 3).

We initially postulated that a delay in intramembranous ossification during *Mmp9*$^{-/-}$ fracture healing was due to a primary defect in cartilage removal, which indirectly delayed subsequent bone formation. An alternative possibility was that the delay in intramembranous ossification represented a separate, and primary, defect in bone formation. To resolve this issue, we developed another model of skeletal repair that allowed us to evaluate whether *Mmp9*$^{-/-}$ bones would heal properly if the primary mode of repair was intramembranous ossification. This repair model was based on the clinical observation that immobilized fractures heal with little or no cartilage, and instead form bone through the direct differentiation of skeletal progenitor cells into osteoblasts (Carter and Giori, 1991; Probst and Spiegel, 1997; Thompson et al., 2002). We stabilized wild-type and *Mmp9*$^{-/-}$ tibiae with an external device that immobilized the fractured bone segments (Thompson et al., 2002), then assessed the calluses for the onset of osteoblast differentiation after 7, 10, 14 and 21 days. As expected, the majority of wild-type calluses formed bone without evidence of chondrogenesis (81%, n=31; Fig. 4A). By contrast, the majority of *Mmp9*$^{-/-}$ mice exhibited late onset, and low expression, of *Oc*, indicating that intramembranous ossification was greatly delayed in the mutant mice (88%, n=16; Fig. 4A). However, more surprising was the fact that skeletal progenitor cells in the *Mmp9*$^{-/-}$ calluses were not simply delayed in their differentiation to osteoblasts. Instead, the cells differentiated into chondrocytes despite the fact that the bone ends were immobilized (Fig. 4A).

The *Mmp9*$^{-/-}$ stabilized fracture phenotype may arise because skeletal progenitor cells are mis-specified to a chondrogenic cell fate, or are delayed in their differentiation to an osteogenic lineage. However, the source(s) of these skeletal progenitor cells was unclear. Because periosteum and endosteum are both probable repositories of skeletal progenitor cells (Einhorn, 1998; Pechak et al., 1986), we sought to localize the cell lineage/differentiation defect to *Mmp9*$^{-/-}$ periosteum or endosteum. We devised another skeletal repair model to test whether periosteal or endosteal regeneration was compromised in *Mmp9*$^{-/-}$ mice by inserting an implant that penetrated both tibial cortices and the bone marrow cavity (Fig. 4B). This repair model injured both tissues, but essentially compartmentalized periosteal regeneration from endosteal repair by blocking the space between the two tissues with the implanted pin. In wild-type animals, new bone formed in the periosteum and endosteum at the implant site, with no evidence of *ColIIa* expression or proteoglycan staining in either location (91%, n=11; Fig. 4B). These findings confirmed that pin implant sites healed through intramembranous ossification. By contrast, abundant cartilage formed at the *Mmp9*$^{-/-}$ implant site (54%, n=13; Fig. 4B), similar to the stabilized fracture phenotype we had observed previously. However, the cartilage was located at the periosteal surface rather than in the endosteum. These data suggested that skeletal progenitor cells in the periosteum are particularly susceptible to the *Mmp9*-null mutation, and either are delayed in their differentiation into osteoblasts, or are misdirected in their cell fate specification.

The pin implant model thus uncovered a potential new role for MMP9 in the commitment of skeletal progenitor cells to an osteogenic lineage. We reasoned that if MMP9 was involved in such a cell fate specification, the protein should be expressed at the time when such decisions are made during fracture repair. We had already observed that cells within the fracture site express chondrogenic and osteogenic markers within 3 days of fracture (Le et al., 2001); using a functional approach we now demonstrated that cells became specified in their fate

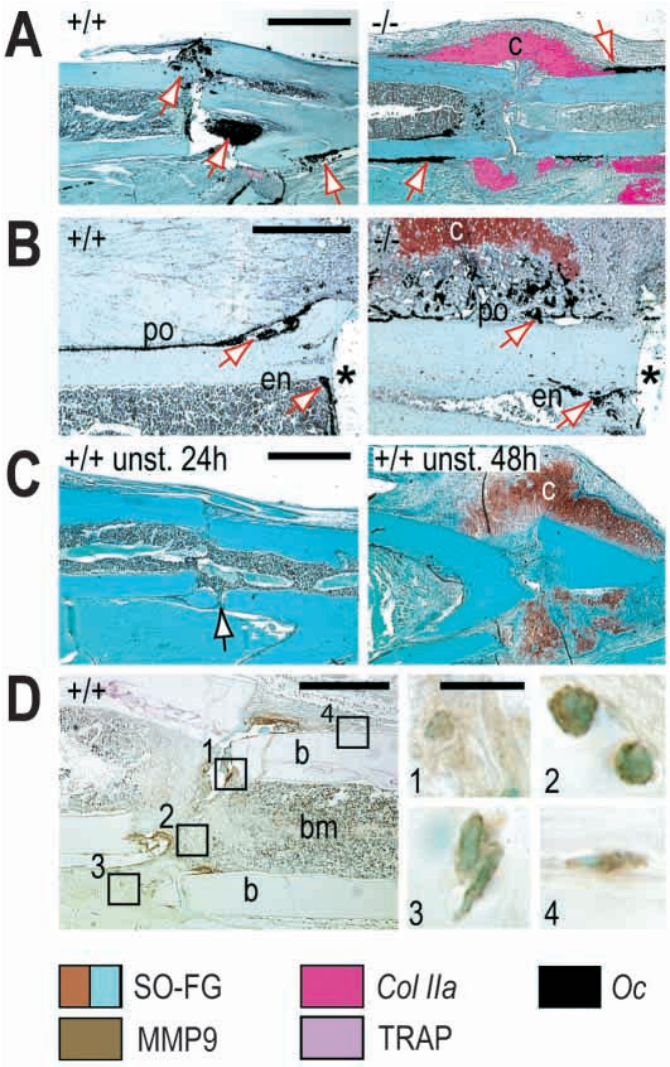

Fig. 4. *Mmp9*$^{-/-}$ mice exhibit an ossification defect during stabilized fracture repair. In A and B, wild-type is left, *Mmp9*$^{-/-}$ is right. (A) SO-FG stained sections through the stabilized fracture site at 10 days confirm the presence of abundant new bone (arrows indicate *Oc* expression) and the absence of cartilage in the wild-type callus (no *ColIIa* signal is evident despite hybridization with this RNA probe). By sharp contrast, abundant cartilage forms in the *Mmp9*$^{-/-}$ callus regardless of stabilization of the bone segments, as shown by the expression of *ColIIa* (pink). *Oc* expression (black) is also detected in the periosteum, adjacent to the fracture site (arrows) and in the endosteum. (B) SO-FG staining of sections at a pin implant (*) at 10 days shows that although no cartilage is detected in wild-type animals, abundant cartilage (red) is present in *Mmp9*$^{-/-}$ animals. This cartilage is restricted to the periosteal surface (po). *Oc* expression (black) is localized both at the periosteal and endosteal (en) surfaces (arrows) in wild-type and *Mmp9*$^{-/-}$ animals. (C) SO-FG stained sections through the wild-type callus illustrate that if fractures are left unstable for 24 hours (left, 24h) and subsequently stabilized, they heal without evidence of cartilage (10 days; arrow indicates the healing fracture). However, fractures that are unstable for 48 hours (right, 48h) and subsequently stabilized tend to heal with abundant cartilage (red). (D) MMP9 immunostaining and double-staining with TRAP illustrate that MMP9 protein (brown) is detected by day 3 in the endosteal matrix (box 1), in inflammatory cells (box 2), in mesenchymal cells within the fracture gap and surrounding soft tissues (box 3), and in the periosteum (box 4). These MMP9-positive cells are TRAP-negative. TRAP-positive osteoclasts/chondroclasts are present at the epiphyseal growth plates of the fractured bone (not shown), and in the cortical bone. bm, bone marrow; c, cortex. Scale bars: in A,C, 1 mm; in B,D (low magnification), 500 μm; in D (high magnification), 10 μm.

within this same time frame. By permitting motion at the site of a fracture for 0, 24 or 48 hours, or for 5 days, and subsequently stabilizing the bone segments until day 10, we were able to show that healing occurred by endochondral ossification if they were mobile for longer than 48 hours (Fig. 4C). Fractures unstable for 24 hours or less healed by intramembranous ossification (Fig. 4C).

These functional data strongly suggested that skeletal progenitor cells could commit to a chondrogenic or an osteogenic fate within 48 to 72 hours following injury. We used immunohistochemistry to show that MMP9 protein was expressed within that same time frame. MMP9 protein was detected in TRAP-negative mesenchymal cells located on the endosteal and periosteal surfaces of the fractured tibia, in the extracellular matrix surrounding the fracture site (Fig. 4D), and in TRAP-negative inflammatory cells such as neutrophils (Fig. 4D). After 5 days, we also detected MMP9 in TRAP-positive pre-osteoclasts (Figs 1, 5) (Engsig et al., 2000). Taken together these data indicate that MMP9 protein is expressed at sites where skeletal progenitor cells are proposed to exist, and that MMP9 is expressed during the period when these cells adopt and commit to chondrogenic or osteogenic fates following injury.

The *Mmp9*$^{-/-}$ fracture repair defect is caused by delayed vascularization of the cartilage callus

The delayed repair defect in *Mmp9*$^{-/-}$ mice resembles a hypertrophic non-union, a human condition characterized by persistent hypertrophic cartilage that is attributed to disruptions in the vascular network of the fracture callus (Einhorn, 1999). Based on the similarities between the mouse phenotype and the human condition, we investigated the extent to which vascularization was compromised in the *Mmp9*$^{-/-}$ callus. Because extracellular matrix remodeling and angiogenesis are closely linked during skeletal tissue development, we included molecular markers of both in this analysis. By 10 days post-fracture, the periphery of the wild-type callus was surrounded by MMP9-expressing, TRAP-positive osteoclasts, but these cells were absent from the *Mmp9*$^{-/-}$ callus (Fig. 5A). By day 14, osteoclasts had removed most of the wild-type cartilage callus and new bone occupied the space (Fig. 5A). By contrast, very few osteoclasts were detectable in the *Mmp9*$^{-/-}$ unremodeled cartilage callus (Fig. 5A). This failure to recruit TRAP-positive cells to the *Mmp9*$^{-/-}$ callus was paralleled by a delay in vascular invasion. Whereas PECAM-positive endothelial cells had accumulated at the periphery of the wild-type hypertrophic cartilage callus, very few endothelial cells were found adjacent to the *Mmp9*$^{-/-}$ hypertrophic cartilage (Fig. 5A). By day 14, endothelial cells invaded the wild-type callus cartilage, whereas in the *Mmp9*$^{-/-}$ callus the endothelial cells remained restricted to the periphery (Fig. 5A).

A delay in endothelial cell recruitment could indicate a delay in cartilage calcification. We performed a series of molecular and histological analyses to test this possibility, but failed to

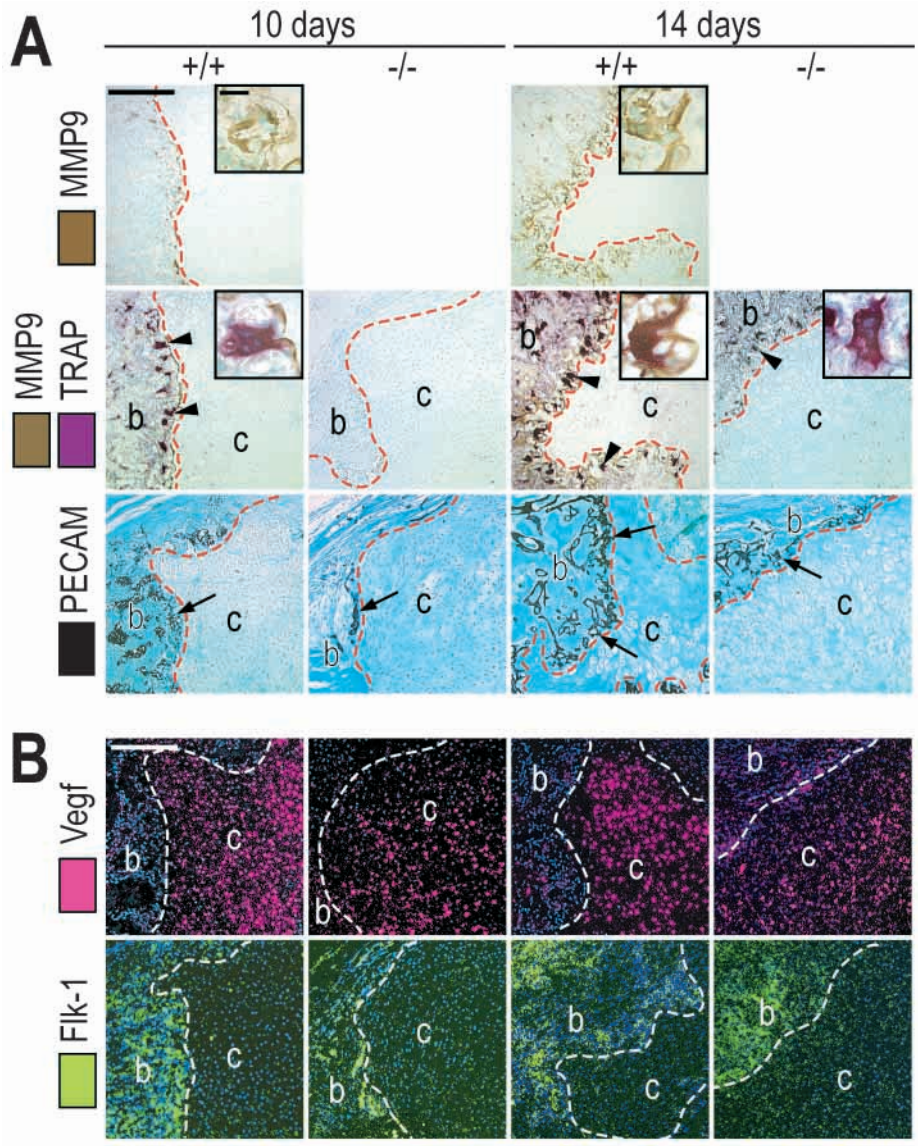

Fig. 5. *Mmp9*$^{-/-}$ fracture healing is hindered by the reduction in chondroclasts/osteoclasts and a delay in vascular invasion. 10 days, left half; 14 days right half. (A) Top row, left panels show that in wild-type mice at 10 days post-fracture, *Mmp9*-expressing chondroclasts/osteoclasts (inset shows cells with characteristic ruffled borders) begin to accumulate at the wild-type cartilage/bone boundary (dotted red line). MMP9 is not expressed in null-mutant mice. In an adjacent section (middle row, left panels), TRAP activity highlights the location of osteoclasts in the wild-type callus (arrowheads), which are largely absent from the *Mmp9*$^{-/-}$ callus. b, bone; c, cartilage. In near-adjacent sections (bottom row, left panels), PECAM-expressing endothelial cells (arrow) have accumulated at the border between wild-type hypertrophic cartilage (c) and newly forming bone (b; arrow). Few PECAM-positive cells are detected in the *Mmp9*$^{-/-}$ callus (arrow). By 14 days post-fracture, abundant MMP9 protein (upper right panels, brown) and TRAP activity (middle right panels, arrowheads) indicate that osteoclasts-mediated degradation of the cartilage callus is well underway (dotted red line indicates the cartilage-bone junction). This degradation activity is associated with increased vascular invasion as illustrated by PECAM-expressing endothelial cells (arrows). Although more PECAM-positive cells are present at 14 days in the *Mmp9*$^{-/-}$ callus (arrow), they are restricted to the edge of the cartilage-bone junction (dotted red line). (B) Tissue sections adjacent to those analyzed in A were examined for the expression of *Vegf* (top, fuchsia) and one of its receptors, *Flk1* (bottom, green). *Vegf* transcripts were detected in late hypertrophic chondrocytes in both wild-type and *Mmp9*$^{-/-}$ calluses at 10 and 14 days post-fracture. Transcripts for *Flk1* were detected in endothelial cells surrounding the cartilage callus of both wild-type and *Mmp9*$^{-/-}$ calluses. b, bone; c, cartilage. The dotted lines in B delimit the boundary of the cartilage in the callus. Scale bars: in A (low magnification) and in B, 200 μm; in A (high magnification), 20 μm.

detect any defect in cartilage matrix mineralization (Fig. 3, and data not shown). Another explanation for the *Mmp9*$^{-/-}$-dependent delay in vascular invasion might be the lack, or decreased expression, of an angiogenic signal or some part of the angiogenic signaling machinery. We examined *Mmp9*$^{-/-}$ calluses at multiple time points during fracture repair for changes in the expression of *Vegf* and the VEGF receptors *Flt1, Flk1 and* neuropilin 1 and *2*. All of these molecules were expressed within the *Mmp9*$^{-/-}$ callus (Fig. 5B, and data not shown). The only difference we detected was in levels of expression: the number of cells expressing *Vegf* was actually higher in the *Mmp9*$^{-/-}$ callus, which was due to the persistence of *Vegf*-positive hypertrophic cartilage (Fig. 5B) (see Colnot and Helms, 2001). We also noted reduced *Flk1* expression, reflecting the paucity of endothelial cells in the *Mmp9*$^{-/-}$ callus (Fig. 5B). Collectively, these data indicated that the *Mmp9*$^{-/-}$ angiogenic defect was not caused by the failure of expression of a potent angiogenic stimulator or its receptors during skeletal repair. Another possible explanation was that MMP9 might be regulating the bioavailability of VEGF, as it does during some disease processes (Bergers et al., 2000).

Exogenous VEGF rescues the *Mmp9*-dependent skeletal repair defect

We reasoned that if functional VEGF is limiting during *Mmp9*$^{-/-}$ skeletal repair, then exogenously applied VEGF should rescue the *Mmp9*$^{-/-}$ defect. We injected recombinant human VEGF protein (rVEGF), or PBS as a control, into the fracture site of *Mmp9*$^{-/-}$ mice, beginning on day 6 (the time at which *Vegf* is normally expressed in the callus), then daily for three more days. We then compared the callus tissues of *Mmp9*$^{-/-}$ mice that received rVEGF with those that received PBS. By 14 days, we noted a clear difference between the two groups: *Mmp9*$^{-/-}$ calluses treated with rVEGF had significantly less cartilage than the controls (Fig. 6A,B). Not only did rVEGF injection reduce the amount of hypertrophic cartilage

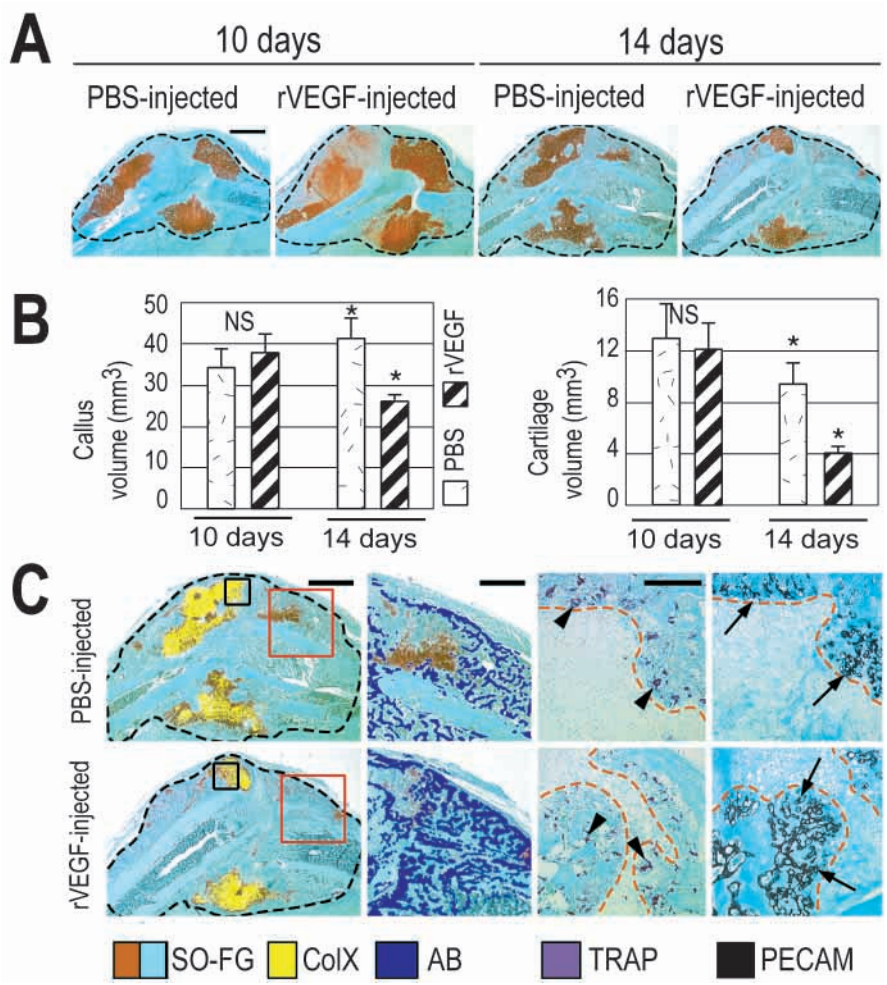

Fig. 6. rVEGF rescues the *Mmp9*$^{-/-}$ fracture repair defect. (A) Tissue sections from PBS- and rVEGF-injected *Mmp9*$^{-/-}$ calluses were stained with SO-FG at 10 and 14 days post-fracture to illustrate that, during the maturation phase of fracture healing (10 days), there is no difference in either the amount of cartilage (red) or the size of the callus (indicated by dotted black line). However, by 14 days post-fracture, the amount of cartilage was substantially reduced in *Mmp9*$^{-/-}$ mice that received rVEGF compared with those that received PBS. These histological observations were confirmed by histomorphometric measurements of the total callus volume and the cartilage volume (B). By 14 days post-fracture, there was a statistically significant decrease in both the total callus volume (left graft, asterisks) and in the cartilage volume (right graft, asterisks) of *Mmp9*$^{-/-}$ mice that received rVEGF (n=10) versus PBS (n=10), as assessed by ANOVA (P=0.03 and P=0.02, respectively; bars represent mean±s.e.m.). (C) By 14 days post-fracture, substantially less hypertrophic cartilage was detected in the *Mmp9*$^{-/-}$ calluses that had been treated with rVEGF compared with their PBS counterparts. Left panels show the yellow *ColX* hybridization signal superimposed upon a tissue section stained with SO-FG. Higher magnification of area boxed in red illustrates that ossification was also accelerated by rVEGF when compared with PBS controls [Analine Blue, (AB) stain superimposed upon an adjacent tissue section stained with SO-FG]. Higher magnification of the area boxed in black illustrates that rVEGF induced substantially greater osteoclast-mediated degradation of the callus compared with PBS controls (arrowheads in upper and lower panels indicate TRAP immunostaining, red dotted line demarcates the boundary between the remaining hypertrophic cartilage and the newly forming bone). Higher magnification of this same region demonstrates that rVEGF resulted in an increased vascular invasion of the callus, as shown by the presence of PECAM-positive endothelial cells penetrating the *Mmp9*$^{-/-}$ hypertrophic cartilage callus (arrows, bottom right panel). Conversely, endothelial cells remain at the periphery of the PBS-injected *Mmp9*$^{-/-}$ callus. Scale bars: in A,C (SO/*ColX* panel), 1 mm; in C (TRAP and PECAM panels), 200 μm.

(*ColX*; Fig. 6C), it also resulted in an increased synthesis of bone matrix (Fig. 6C, boxed area in red, AB). rVEGF treatment also resulted in an increase in TRAP activity (Fig. 6C) and in the numbers of endothelial cells that invaded the *Mmp9*$^{-/-}$ callus (Fig. 6C, arrows). These observations demonstrated that rVEGF compensated for the lack of *Mmp9* by stimulating the recruitment/and or differentiation of the three cell types that express the VEGF receptor: chondroclasts/osteoclasts that remodel hypertrophic cartilage, endothelial cells that form vascular channels, and osteoblasts that generate new bone at the injury site.

DISCUSSION

Fetal skeletogenesis and adult skeletal repair: two sides of the same coin?

The similarities between *Mmp9*$^{-/-}$ skeletal defects that emerge during fetal development and those that occur during adult repair offer the strongest evidence to date that the same molecular mechanisms are employed to achieve bone formation, regardless of age. At a histological level, fracture healing closely resembles fetal skeletal development. Mesenchymal cells alter their extracellular matrix and cell-cell contacts, and aggregate, thus forming condensations that will either form cartilage or bone (Le et al., 2001; Probst and Spiegel, 1997). The molecular programs regulating chondrogenesis and osteogenesis are also conserved (Ferguson et al., 1999; Vortkamp et al., 1998). These observations have led us and others to hypothesize that fracture healing recapitulates fetal skeletogenesis (Ferguson et al., 1998; Vortkamp et al., 1998). However, the differences between a fetal developmental program and an adult reparative process cannot be underestimated. Inflammation plays a crucial role in healing, as do mechanical forces that act upon cells in the fracture callus (Carter et al., 1998; Einhorn et al., 1995). The presence, or paucity, of stem cells in an adult, and their developmental potency, is certain to influence adult healing as well. The contributions of these factors to skeletal tissue regeneration remain largely unknown and most probably under appreciated. We undertook this study to gain an appreciation for the roles of one MMP in the

process of skeletal tissue formation. Our previous work had uncovered a role for MMP9 in fetal skeletogenesis (Vu et al., 1998), and in this study we elucidated additional functions for MMP9 in adult skeletal repair.

MMP9 regulates hypertrophic cartilage angiogenesis

Our data indicate that MMP9 stimulates angiogenesis of the hypertrophic cartilage callus (Fig. 5). One model that may account for the *Mmp9*$^{-/-}$ repair defect is that the loss of MMP9 affects the bioavailability of a potent angiogenic molecule, VEGF. The fact that VEGF cannot accelerate healing in wild-type animals (data not shown) but can rescue the phenotype of Mmp9$^{-/-}$ mutants indicates that VEGF is a limiting factor in the absence of MMP9, which suggests an interaction between the two molecules. MMP9 may regulate vascular invasion by releasing VEGF that is bound to the hypertrophic cartilage matrix. Once released, VEGF could bind to its receptors on endothelial cells, osteoclasts and osteoblasts (Nakagawa et al., 2000; Risau, 1997), stimulating their migration and activity at the fracture site. Precisely how MMP9 and VEGF coordinate the activity of three cell types (osteoblasts, osteoclasts/chondroclasts and endothelial cells) during the process of skeletal repair is still a puzzle. Other angiogenic factors are clearly involved in skeletal repair, as the *Mmp9*$^{-/-}$ defect is transient (Fig. 2). Likewise, other proteases may mediate angiogenic activity (Yamagiwa et al., 1999), as is suggested by skeletal defects in *Mt1-Mmp*$^{-/-}$ mice (Holmbeck et al., 1999). Understanding the identities and contributions of other angiogenic regulators and proteases will undoubtedly provide a more complete view of how extracellular matrix remodeling and angiogenesis are synchronized during skeletal tissue regeneration.

MMP9 mediates an angiogenic switch during bone regeneration

The transition of an anti-angiogenic tissue, cartilage, to an angiogenic one, bone, is a crucial feature of adult bone regeneration (Fig. 5). Tumors undergo a similar angiogenic switch, heralding their progression to a more aggressive form of the disease (Bergers et al., 2000; Huss et al., 2001; Semenza, 2000). Angiogenic switches also occur during the development of other tissues, such as the lung and the mammary gland (Muratore et al., 2000; Pepper et al., 2000).

During fracture healing, a failure of cartilage to undergo an angiogenic switch is associated with a pathological skeletal condition known as hypertrophic non-union. The *Mmp9*$^{-/-}$ fracture healing phenotype is a prime example of how a genetic mutation can impair adult healing in a phenotypically normal individual. As illustrated by the *Mmp9*$^{-/-}$ mouse, a complete loss of MMP9 can be compatible with life and normal reproduction; humans with mutations in MMP2 are also viable (Martignetti et al., 2001). It will be interesting to ascertain if a genetic predisposition underlies human skeletal healing defects that are associated with perturbations in vascular remodeling, and if biologically based therapies can be developed for the treatment of such recalcitrant skeletal injuries.

MMP9 and cell fate specification

MMP9 plays another role during the early phase of stabilized skeletal repair. Although stabilized skeletal injuries heal through intramembranous ossification in wild-type mice, the same injuries heal through endochondral ossification in *Mmp9*$^{-/-}$ mice (Fig. 4). There are a number of possible explanations for this curious phenotype. For example, MMP9 may participate in the mobilization of osteoprogenitor cells from the periosteum and/or from the bone marrow. In the bone marrow, MMP9 is involved in the mobilization and activation of hematopoietic and endothelial stem cells, and MMP9-expessing cells may in fact share a common lineage with these cells (Heissig et al., 2002). The *Mmp9*$^{-/-}$ intramembranous ossification defect may therefore be cause by a failure to release and/or activate osteoprogenitor cells from either the periosteum or the bone marrow cavity.

Alternatively, the differentiation of skeletal progenitor cells may be delayed in *Mmp9*$^{-/-}$ stabilized injuries. MMP9 appears to release VEGF from its extracellular matrix stores (Bergers et al., 2000), and a failure to activate one of the VEGF receptors on osteoprogenitor cells (Deckers et al., 2000; Midy and Plouët, 1994) may ultimately affect the rate at which these cells differentiate. As the *Mmp9*$^{-/-}$ ossification defect is transient, it is highly likely that other signals also participate in osteoblast differentiation during repair. The nature of these compensatory signals is, at present, unknown.

Another possibility is that the MMP9 mutation may disrupt the formation of an intact vascular network during the initial stages of stabilized repair. A stable environment has long been thought to favor the formation of an intact vascular network (Claes et al., 2002; Glowacki, 1998), and this oxygen-rich environment appears to support the differentiation of skeletal progenitor cells into osteoblasts. One possibility is that a vascular network fails to form around the *Mmp9*$^{-/-}$ stabilized fracture or the *Mmp9*$^{-/-}$ implant site (Fig. 3). However, we think this is the least likely explanation, as rVEGF failed to rescue the *Mmp9*$^{-/-}$ stabilized healing defect. Other angiogenic molecules, such as CTGF, the angiopoietins (Street et al., 2002; Thurston et al., 1999) and the fibroblast growth factors (Kawaguchi et al., 1994), may regulate the establishment of a vascular network during early stages of fracture healing.

The mechanical environment influences progenitor cell fate decisions

Until recently (Henderson and Carter, 2002), it was thought that the most prominent difference between fetal and adult bone formation was the fact that fetal endochondral ossification takes place independently of mechanical stimuli, whereas the fate of progenitor cells in the fracture callus depends upon the mechanical environment. Clinical examination, biomechanical data (Carter and Giori, 1991; Carter et al., 1998) and biological observations (Claes et al., 1998; Park et al., 2003; Thompson et al., 2002) clearly indicate that stabilization favors the differentiation of cells into osteoblasts, whereas the lack of stabilization leads initially to the production of chondrocytes. In *Mmp9*$^{-/-}$ mice, the majority of progenitor cells in the fracture callus adopt a chondrogenic fate regardless of whether the fracture is stabilized or not. Precisely how the mechanical environment and MMP9 function are coordinated is still open to speculation. The differences in stabilized and non-stabilized fracture healing may be attributable to the extent of tissue disruption, and therefore may not be directly comparable. For example, stabilized fractures and implant models may be characterized by minimal tissue disruption following acute injury,

whereas non-stabilized fractures may be subjected to continued tissue disruption. These differences might trigger signaling pathways that are not induced in a stable mechanical environment and therefore healing between the two models may be difficult to compare. However, there is no current data to support or refute the hypothesis that the extent of mechanical disruption leads to the activation of different molecular pathways.

In vitro studies show that stretch and compression forces applied to tissues from a fracture site upregulate the expression of some MMPs (Haas et al., 1999; Rubin et al., 1999), and this upregulation occurs through cell adhesion molecules, such as integrins (Spessotto et al., 2002; Sugiura and Berditchevski, 1999). Thus it is possible that different MMP-induced responses to varying mechanical stimuli may modulate the activity of different sets of growth factors, analogous to the case of hematopoietic reconstitution (Heissig et al., 2002). Probable candidate growth and differentiation factors include VEGF (Villars et al., 2000), and members of the transforming growth factor β (Alliston et al., 2001; Bonewald and Dallas, 1994; Centrella et al., 1994), bone morphogenetic protein (Fromigue et al., 1998), hedgehog protein (Pola et al., 2001; Spinella-Jaegle et al., 2001) and fibroblast growth factor (Liu et al., 2002; Scutt and Bertram, 1999) families. It is equally probable that subtle shifts in the balance of these and other growth factors subsequently affect the differentiation, or survival and proliferation, of osteo- or chondroprogenitor cells that populate the fracture site.

Inflammation and skeletal repair

Inflammation plays an important role in bone repair (Altman et al., 1995; Banovac et al., 1995; Zhang et al., 2002). The mechanical environment influences the inflammatory response (Hankemeier et al., 2001), although the mechanisms by which this is achieved are unclear. MMP9 participates in the inflammatory response associated with skeletal injury, as demonstrated by the fact that neutrophils and macrophages strongly express the protein in the early fracture callus and in the implant site. The function(s) of MMP9 in the inflammatory response associated with the early stages of skeletal repair is still unclear. MMP9 released from neutrophils, mast cells and macrophages may be involved in remodeling the early fracture callus. Inflammatory cells expressing MMP9 may preferentially accumulate in a stable mechanical environment, which would result in the delivery of more cytokines to these sites of injury. In turn, these cytokines may stimulate osteogenesis to a greater degree than is observed in a non-stabilized fracture.

In conclusion, these data reveal new roles for MMP9 in fracture healing. The continued close scrutiny of the parallels, and differences, between fetal and adult programs of cell differentiation, extracellular matrix remodeling and angiogenesis will surely yield new insights into these crucial events in tissue regeneration.

The authors thank S. Huang and P. Chong for technical assistance; J. Rinkenberger for help generating the *Mmp9*$^{-/-}$ mice; S. Gansky and S. Shain for statistical analyses; N. Ferrara at Genentech Inc. for providing rVEGF protein; and L. de la Fuente, R. Marcucio, N. Ortega, and R. Schneider for helpful comments on the manuscript. Special thanks also to RFG. This work was supported by funds from NIH K08 AR02164 (T.M.), R01 DE31497 (J.A.H.), P60 DE13058 (J.A.H. and Z.W.) and R01 AR46238 (Z.W. and J.A.H.).

REFERENCES

Albrecht, U., Eichele, G., Helms, J. A. and Lin, H. (1997). *Visualization of gene expression patterns by in situ hybridization.* Boca Raton, FL: CRC Press.

Alliston, T., Choy, L., Ducy, P., Karsenty, G. and Derynck, R. (2001). TGF-beta-induced repression of CBFA1 by Smad3 decreases cbfa1 and osteocalcin expression and inhibits osteoblast differentiation. *EMBO J.* **20**, 2254-2272.

Altman, R. D., Latta, L. L., Keer, R., Renfree, K., Hornicek, F. J. and Banovac, K. (1995). Effect of nonsteroidal antiinflammatory drugs on fracture healing: a laboratory study in rats. *J. Orthop. Trauma* **9**, 392-400.

Banovac, K., Renfree, K., Makowski, A. L., Latta, L. L. and Altman, R. D. (1995). Fracture healing and mast cells. *J. Orthop. Trauma* **9**, 482-490.

Bergers, G., Brekken, R., McMahon, G., Vu, T. H., Itoh, T., Tamaki, K., Tanzawa, K., Thorpe, P., Itohara, S., Werb, Z. et al. (2000). Matrix metalloproteinase-9 triggers the angiogenic switch during carcinogenesis. *Nat. Cell Biol.* **2**, 737-744.

Bonewald, L. F. and Dallas, S. L. (1994). Role of active and latent transforming growth factor beta in bone formation. *J. Cell. Biochem.* **55**, 350-357.

Bruder, S. P., Fink, D. J. and Caplan, A. I. (1994). Mesenchymal stem cells in bone development, bone repair, and skeletal regeneration therapy. *J. Cell. Biochem.* **56**, 283-294.

Carter, D. C. and Giori, N. J. (1991). *Effect of mechanical stress on tissue differentiation in the bony implant bed*. Toronto: University of Toronto Press.

Carter, D. R., Beaupré, G. S., Giori, N. J. and Helms, J. A. (1998). Mechanobiology of skeletal regeneration. *Clinical Orthop. Relat. Res. Suppl.* **355**, S41-S55.

Centrella, M., Horowitz, M. C., Wozney, J. M. and McCarthy, T. L. (1994). Transforming growth factor-beta gene family members and bone. *Endocr. Rev.* **15**, 27-39.

Claes, L., Eckert-Hubner, K. and Augat, P. (2002). The effect of mechanical stability on local vascularization and tissue differentiation in callus healing. *J. Orthop. Res.* **20**, 1099-1105.

Claes, L. E., Heigele, C. A., Neidlinger-Wilke, C., Kaspar, D., Seidl, W., Margevicius, K. J. and Augat, P. (1998). Effects of mechanical factors on the fracture healing process. *Clin. Orthop. Rel. Res. Suppl.* **355**, S132-S147.

Colnot, C. I. and Helms, J. A. (2001). A molecular analysis of matrix remodeling and angiogenesis during long bone development. *Mech. Dev.* **100**, 245-250.

Deckers, M., Karperien, M., van der Bent, C., Yamashita, T., Papapoulos, S. and Lowik, C. (2000). Expression of vascular endothelial growth factors and their receptors during osteoblast differentiation. *Endocrinology* **141**, 1667-1674.

Einhorn, T. A. (1998). The cell and molecular biology of fracture healing. *Clin. Orthop. Rel. Res. Suppl.* **355**, S7-S21.

Einhorn, T. A. (1999). Clinically applied models of bone regeneration in tissue engineering research. *Clin. Orthop. Rel. Res. Suppl.* **367**, S59-S67.

Einhorn, T. A., Majeska, R. J., Rush, E. B., Levine, P. M. and Horowitz, M. C. (1995). The expression of cytokine activity by fracture callus. *J. Bone Miner. Res.* **10**, 1272-1281.

Ekholm, E., Hankenson, K. D., Uusitalo, H., Hiltunen, A., Gardner, H., Heino, J. and Penttinen, R. (2002). Diminished callus size and cartilage synthesis in alpha 1 beta 1 integrin-deficient mice during bone fracture healing. *Am. J. Pathol.* **160**, 1779-1785.

Engsig, M. T., Chen, Q., Vu, T. H., Pedersen, A., Therdkidsen, B., Lund, L. R., Henriksen, T., Lenhard, T., Foged, N. T., Werb, Z. et al. (2000). Matrix metalloproteinase 9 and vascular endothelial growth factor are essential for osteoclast recruitment into developing long bones. *J. Cell Biol.* **151**, 1-11.

Ferguson, C. M., Miclau, T., Hu, D., Alpern, E. and Helms, J. A. (1998). Common molecular pathways in skeletal morphogenesis and repair. *Ann. New York Acad. Sci.* **857**, 33-42.

Ferguson, C., Alpern, E., Miclau, T. and Helms, J. A. (1999). Does adult fracture repair recapitulate embryonic skeletal formation? *Mech. Dev.* **87**, 57-66.

Fromigue, O., Marie, P. J. and Lomri, A. (1998). Bone morphogenetic protein-2 and transforming growth factor-beta(2) interact to modulate human bone marrow stromal cell proliferation and differentiation. *J. Cell. Biochem.* **68**, 411-426.

Glowacki, J. (1998). Angiogenesis in fracture repair. *Clin. Orthop. Relat. Res. Suppl.* **355**, S82-S89.

Haas, T. L., Stitelman, D., Davis, S. J., Apte, S. S. and Madri, J. A.

(1999). Egr-1 mediates extracellular matrix-driven transcription of membrane type 1 matrix metalloproteinase in endothelium. *J. Bio. Chem.* **274**, 22679-22685.

Hall, B. K. (1988). The embryonic development of bone. *Am. Sci.* **76**, 174-181.

Hankemeier, S., Grassel, S., Plenz, G., Spiegel, H. U., Bruckner, P. and Probst, A. (2001). Alteration of fracture stability influences chondrogenesis, osteogenesis and immigration of macrophages. *J. Orthop. Res.* **19**, 531-538.

Heissig, B., Hattori, K., Dias, S., Ferris, B., Friedrich, M., Hackett, N. R., Lyden, D., Wood, J., Crystal, R. G., Moore, M. A. S. et al. (2002). Recruitment of stem and progenitor cells from the bone marrow niche requires MMP-9-mediated release of Kit ligand. *Cell* **109**, 625-637.

Henderson, J. H. and Carter, D. R. (2002). Mechanical induction in limb morphogenesis: the role of growth-generated strains and pressures. *Bone* **31**, 645-653.

Hiltunen, A., Aro, H. T. and Vuorio, E. (1993). Regulation of extracellular matrix genes during fracture healing in mice. *Clin. Orthop. Relat. Res.* **46**, 23-27.

Holmbeck, K., Bianco, P., Caterina, J., Yamada, S., Kromer, M., Kuznetsov, S. A., Mankani, M., Robey, P. G., Poole, A. R., Pidoux, I. et al. (1999). MT1-MMP-deficient mice develop dwarfism, osteopenia, arthritis, and connective tissue disease due to inadequate collagen turnover. *Cell* **99**, 81-92.

Huss, W. J., Hanrahan, C. F., Barrios, R. J., Simons, J. W. and Greenberg, N. M. (2001). Angiogenesis and prostate cancer: identification of a molecular progression switch. *Cancer Res.* **61**, 2736-2743.

Karsenty, G. and Wagner, E. F. (2002). Reaching a genetic and molecular understanding of skeletal development. *Dev. Cell* **2**, 389-406.

Kawaguchi, H., Kurokawa, T., Hanada, K., Hiyama, Y., Tamura, M., Ogata, E. and Matsumoto, T. (1994). Stimulation of fracture repair by recombinant human basic fibroblast growth factor in normal and streptozotocin-diabetic rats. *Endocrinology* **135**, 774-781.

Le, A. X., Miclau, T., Hu, D. and Helms, J. A. (2001). Molecular aspects of healing in stabilized and non-stabilized fractures. *J. Orthop. Res.* **19**, 78-84.

Lian, J. B., Hauschka, P. V. and Gallop, P. M. (1978). Properties and biosynthesis of a vitamin K-dependent calcium binding protein in bone. *Fed. Proc.* **37**, 2615-2620.

Liu, Z., Xu, J., Colvin, J. S. and Ornitz, D. M. (2002). Coordination of chondrogenesis and osteogenesis by fibroblast growth factor 18. *Genes Dev.* **16**, 859-869.

Martignetti, J. A., Al Aqeel, A., Al Sewairi, W., Boumah, C. E., Kambouris, M., Al Mayouf, S., Sheth, K. V., Al Eid, W., Dowling, O., Harris, J. et al. (2001). Mutation of the matrix metalloproteinase 2 gene (MMP2) causes a multicentric osteolysis and arthritis syndrome. *Nat. Genet.* **28**, 261-265.

Midy, V. and Plouët, J. (1994). Vasculotropin/vascular endothelial growth factor induces differentiation in cultured osteoblasts. *Biochem. Biophys. Res. Commun.* **199**, 380-386.

Muratore, C. S., Nguyen, H. T., Ziegler, M. M. and Wilson, J. M. (2000). Stretch-induced upregulation of VEGF gene expression in murine pulmonary culture: a role for angiogenesis in lung development. *J. Pediatr. Surg.* **35**, 906-913.

Nakagawa, M., Kaneda, T., Arakawa, T., Morita, S., Sato, T., Yomada, T., Hanada, K., Kumegawa, M. and Hakeda, Y. (2000). Vascular endothelial growth factor (VEGF) directly enhances osteoclastic bone resorption and survival of mature osteoclasts. *FEBS Lett.* **473**, 161-164.

Park, S. H., O'Connor, K. M. and McKellop, H. (2003). Interaction between active motion and exogenous transforming growth factor beta during tibial fracture repair. *J. Orthop. Trauma* **17**, 2-10.

Pechak, D. G., Kujawa, M. J. and Caplan, A. I. (1986). Morphological and histochemical events during first bone formation in embryonic chick limbs. *Bone* **7**, 441-458.

Pepper, M. S., Baetens, D., Mandriota, S. J., Di Sanza, C., Oikemus, S., Lane, T. F., Soriano, J. V., Montesano, R. and Iruela-Arispe, M. L. (2000). Regulation of VEGF and VEGF receptor expression in the rodent mammary gland during pregnancy, lactation, and involution. *Dev. Dyn.* **218**, 507-524.

Pola, R., Ling, L. E., Silver, M., Corbley, M. J., Kearney, M., Pepinsky, R. B., Shapiro, R., Taylor, F. R., Baker, D. P., Asahara, T. et al. (2001). The morphogen Sonic hedgehog is an indirect angiogenic agent upregulating two families of angiogenic growth factors. *Nat. Med.* **7**, 706-711.

Probst, A. and Spiegel, H. U. (1997). Cellular mechanisms of bone repair. *J. Invest. Surg.* **10**, 77-86.

Risau, W. (1997). Mechanisms of angiogenesis. *Nature* **386**, 671-674.

Rubin, C., Sun, Y. Q., Hadjiargyrou, M. and McLeod, K. (1999). Increased expression of matrix metalloproteinase-1 in osteocytes precedes bone resorption as stimulated by disuse: evidence for autoregulation of the cell's mechanical environment? *J. Orthop. Res.* **17**, 354-361.

Sandell, L. J., Zhu, Y. and Oganesian, A. (1997). *Collagen gene expression as markers for skeletal development, disease, and repair*. Rosemont, IL: American Academy of Orthopedic Surgeons.

Scutt, A. and Bertram, P. (1999). Basic fibroblast growth factor in the presence of dexamethasone stimulates colony formation, expansion, and osteoblastic differentiation by rat bone marrow stromal cells. *Calcif. Tissue Int.* **64**, 69-77.

Semenza, G. L. (2000). HIF-1: using two hands to flip the angiogenic switch. *Cancer Metastasis Rev.* **19**, 59-65.

Simon, A. M., Manigrasso, M. B. and O'Connor, J. P. (2002). Cyclo-oxygenase 2 function is essential for bone fracture healing. *J. Bone Miner. Res.* **17**, 963-976.

Spessotto, P., Rossi, F. M., Degan, M., Di Francia, R., Perris, R., Colombatti, A. and Gattei, V. (2002). Hyaluronan-CD44 interaction hampers migration of osteoclast-like cells by down-regulating MMP-9. *J. Cell Biol.* **158**, 1133-1144.

Spinella-Jaegle, S., Rawadi, G., Kawai, S., Gallea, S., Faucheu, C., Mollat, P., Coutois, B., Bergaud, B., Ramez, V., Banchet, A. M. et al. (2001). Sonic hedgehog increases the commitment of pluripotent mesenchymal cells into the osteoblastic lineage and abolishes adipocytic differentiation. *J. Cell Sci.* **114**, 2085-2094.

Street, J., Bao, M., deGuzman, L., Bunting, S., Peale, F. V., Jr, Ferrara, N., Steinmetz, H., Hoeffel, J., Cleland, J. L., Daugherty, A. et al. (2002). Vascular endothelial growth factor stimulates bone repair by promoting angiogenesis and bone turnover. *Proc. Natl. Acad. Sci. USA* **99**, 9656-9661.

Sugiura, T. and Berditchevski, F. (1999). Function of alpha 3 beta 1-tetraspanin protein complexes in tumor cell invasion. Evidence for the role of the complexes in production of matrix metalloproteinase 2 (MMP-2). *J. Cell Biol.* **146**, 1375-1389.

Tay, B. K., Le, A. X., Gould, S. E. and Helms, J. A. (1998). Histochemical and molecular analyses of distraction osteogenesis in a mouse model. *J. Orthop. Res.* **16**, 636-642.

Thompson, Z., Miclau, T., Hu, D. and Helms, J. A. (2002). A model for intramembranous ossification during fracture healing. *J. Orthop. Res.* **20**, 1091-1098.

Thurston, G., Suri, C., Smith, K., McClain, J., Sato, T. N., Yancopoulos, G. D. and McDonald, D. M. (1999). Leakage-resistant blood vessels in mice transgenically overexpressing angiopoietin-1. *Science* **286**, 2511-2514.

Villars, F., Bordenave, L., Bareille, R. and Amedee, J. (2000). Effect of human endothelial cells on human bone marrow stromal cell phenotype: role of VEGF? *J. Cell. Biochem.* **74**, 672-685.

Vortkamp, A., Pathi, S., Peretti, G. M., Caruso, E. M., Zaleske, D. J. and Tabin, C. J. (1998). Recapitulation of signals regulating embryonic bone formation during postnatal growth and in fracture repair. *Mech. Dev.* **71**, 65-76.

Vu, T. H., Shipley, J. M., Bergers, G., Berger, J. E., Helms, J. A., Hanahan, D., Shapiro, S. D., Senior, R. M. and Werb, Z. (1998). MMP-9/gelatinase B is a key regulator of growth plate angiogenesis and apoptosis of hypertrophic chondrocytes. *Cell* **93**, 411-422.

White, A. A., III, Panjabi, M. M. and Southwick, W. O. (1977). The four biomechanical stages of fracture repair. *J. Bone Joint Surg. Am.* **59**, 188-192.

Yamagiwa, H., Tokunaga, K., Hayami, T., Hatano, H., Uchida, M., Endo, N. and Takahashi, H. E. (1999). Expression of metalloproteinase-13 (Collagenase-3) is induced during fracture healing in mice. *Bone* **25**, 197-203.

Zhang, X., Schwarz, E. M., Young, D. A., Puzas, J. E., Rosier, R. N. and O'Keefe, R. J. (2002). Cyclooxygenase-2 regulates mesenchymal cell differentiation into the osteoblast lineage and is critically involved in bone repair. *J. Clin. Invest.* **109**, 1405-1415.